Effect of Alkylation on the Cellular Uptake of Polyethylene Glycol-Coated Gold Nanoparticles

Lok Wai Cola Ho, [†] *Wing-Yin Yung,* [‡] *Kwun Hei Samuel Sy,* [†] *Ho Yin Li,* [§] *Chun Kit K. Choi,* [†] *Ken Cham-Fai Leung,* [‡] *Thomas W.Y. Lee,* [§] *Chung Hang Jonathan Choi*,* [†,⊥]

[†]Department of Electronic Engineering (Biomedical Engineering), [§]School of Pharmacy, [⊥]Shun Hing Institute of Advanced Engineering, The Chinese University of Hong Kong, Shatin, New Territories, and [‡]Department of Chemistry, Hong Kong Baptist University, Kowloon, Hong Kong, China

*Corresponding author: Chung Hang Jonathan Choi: jchchoi@cuhk.edu.hk

KEYWORDS: alkylation, cellular uptake, gold nanoparticles, polyethylene glycol, filopodia

Supplementary Materials and Methods

Detection of Primary Amines by Ninhydrin. 10 μL of 1 mg/mL HS-PEG-CnH2n+1 in water and alkylamine in methanol of different concentrations was spotted onto a TLC plate (Qingdao Kangyexin). The plate was then dried and dipped into a solution of 0.3% ninhydrin (Tokyo Chemical Industry) in n-butanol/acetic acid (100:3, v/v) for 30 s. After removing the excess reagent by a paper towel, the color of Ruhemann's purple was developed by drying the TLC plate with a heat gun for 2 min.

Negative Staining of PEG Coating on AuNPs by Uranyl Acetate. To reveal the presence of the PEG corona on the AuNP surface by transmission electron microscopy (TEM), 10 μL of 2 nM NP solution was drop-cast onto a TEM copper grid (200 mesh; Beijing Zhongjingkeyi Technology) and left for 30 min. After removing the NP solution, 10 μL of 2% uranyl acetate (Sigma) in water was added onto the TEM grid for another 1 min. After removing the uranyl acetate solution, the stained grid was allowed to dry at RT for at least 4 h before visualization under TEM at a beam voltage of 100 kV (Hitachi H7700).

Water/1-Octanol Partitioning of Nanoparticles. 1 mL of 1-octanol (Sigma) and 1 mL of water containing 1 nM of methoxy-PEG-AuNPs or alkyl$_{4\%}$-PEG-AuNPs was added into a glass vial and mixed at 40 rpm by using a tube revolver (Thermo Scientific). After 24 h of mixing, 50 μL of samples was extracted from the aqueous phase. The concentration of the NPs remaining in the aqueous phase was determined by UV-vis spectrophotometry (Agilent Cary 5000).

Western Blotting. siRNA-transfected Kera-308 cells were washed with ice-cold Tris-buffered saline (TBS) buffer twice and scrapped off in 100 μL of Radioimmunoprecipitation assay buffer (RIPA buffer) supplemented with 1× protease cocktail (Thermo Scientific) and 5 mM EDTA (Thermo Scientific). The whole-cell lysate was then clarified by centrifugation for 15 min at 13,200 rpm at 4 °C. Protein concentrations were determined by using the BCA Protein Assay Kit (Pierce). Equal amounts (20 μg) of protein samples were fractionated and transferred to a polyvinylidene fluoride (PVDF) membrane (Bio-Rad) and blocked in 5% blotting grade blocker in TBS with 0.1% Tween20 (Sigma)(TBST). Caveolin-1, clathrin heavy chain-1, and dynamin-2 were probed by rabbit primary antibodies against Cav-1 (5 μg, Cell Signaling Technology, D46G3), Clhc-1 (5 μg, Abcam, ab21679), and Dnm-2 (5 μg Santa Cruz, sc-6400), together with rabbit primary antibodies against β-actin (1.5 μg Abcam, ab8227) in 5 mL of 5% blocker in TBST. The desired bands were detected by HRP-labeled secondary antibodies (Invitrogen goat anti-rabbit IgG (H+L)-HRP cross-adsorbed secondary antibody, G-21234) (5 μg in 5 mL of 5% blocker in TBST). After adding a mixture of peroxide solution (Bio-Rad) and luminol/enhancer solution (Bio-Rad) at a ratio of 1:1 (v/v), the stained bands were visualized by the Chemi-Doc Touch gel imaging system (Bio-Rad).

Cell Viability by Calcein/Propidium Iodide Staining. Kera-308 cells were seeded in a 24-well plate and the cell population was allowed to reach ~80% confluence. During the experiment, cells were incubated with 0.3 mL of 1 nM $alkyl_{x\%}$-PEG-AuNPs formulated in OptiMEM for 24 h. After removing the NPs, the cells were rinsed by phosphate-buffered saline (PBS) twice. 0.2 mL of PBS that contains 0.5 μg/mL calcein-AM (Thermo Scientific) and 3 μg/mL propidium iodide (Thermo Scientific) was incubated with cells for 10 min at 37˚C. After removing the staining solution and rinsing the cells with 0.5 mL of PBS twice, the cells were immersed in 0.3 mL of fresh PBS and

immediately imaged under an inverted fluorescence microscope (Nikon Ti-E). The excitation and emission wavelengths of calcein are 495 and 515 nm, respectively. The excitation and emission wavelengths of propidium iodide are 535 and 617 nm, respectively.

Cell Viability by the AlamarBlue Assay. Kera-308 cells were seeded in a 96-well plate, and the cell population was allowed to reach ~80% confluence before the experiment. During the experiment, cells were incubated with 0.2 mL of OptiMEM that contains either 1 nM alkyl$_{x\%}$-PEG-AuNPs or chemical blockers at various concentrations for 6 h. These blockers include fucoidan (50 μg/mL, Santa Cruz), filipin III (2.5 μg/mL, Sigma), chlorpromazine (5 μg/mL, Tokyo Chemical Industry), amiloride (500 μg/mL, Sigma), cytochalasin D (5 μg/mL, Cayman Chemical), mannan (1 mg/mL, Sigma), dynasore (120 μM, Cayman Chemical), and methyl-beta-cyclodextrin (m-βCD) (10 mM, Tokyo Chemical Industry). After removing the NPs or blockers and rinsing the cells by PBS for 3 times, the alamarBlue reagent (Invitrogen) was used to test the cell viability by measuring the optical absorbance at 570 nm and 600 nm by a Multiskan GO UV-absorbance microplate reader (Thermo Scientific). Reported data represent mean ± SD from four independent experiments.

Supplementary Figures

Table S1 Mass Percentage of Alkyl Groups in the Conventional Lipid-based NPs

Reference	Mole ratios of the NP formulation[a]	Mass percentage of alkyl groups in the total mass of the NP (%)[b]
PEG-liposomes[1]	HEPC: Cholesterol: PEG_{2000}-DSPE = 1.85 : 1.00 : 0.15	42%
Lipid nanoparticles (LNPs)[2]	Ionizable lipid (DLin-MC3-DMA): DSPC: Cholesterol: PEG_{2000}-DMG = 50 : 10 : 38.5 : 1.5	28%
Cholesterol conjugated nanoparticles[3]	PC: Cholesterol: PEG_{2000}-DSPE = 2 : 1 : 0.2	46%
Phospholipid encapsulated quantum dots[4]	PEG_{2000}-PE: DPPC = 4 : 6	26%

[a] Abbreviations: HEPC: Hydrogenated egg phosphatidylcholine; DSPE: 1,2-distearoyl-sn-glycero-3-phosphoethanolamine; DSPC: disteroylphosphatidyl choline; DMG: 1,2-Dimyristoyl-sn-glycerol; PC: L-α -phosphatidylcholine; PE: 1,2-dipalmitoyl-sn-glycero-3-phosphoethanolamine and DPPC: 1,2-dipalmitoyl-glycero-3-phosphocholine.

[b] $$\text{Mass percentage of alkyl groups in the NP formulation} = \frac{(\text{Mass of alkyl group per unit NP formulation})}{(\text{Mass of all constituents per unit NP formulation})} \times 100\%$$

Only the portion of alkyl chains containing 6 or more consecutive carbons are considered in the calculation of alkyl mass. Mass of the drug, siRNA or the inorganic NP core are not taken into account when we calculate the total mass of NP. For the HEPC molecule (780 Da), we count only the mass of its 15- and 17-carbon long alkyl chains (~ 418 Da for both chains). For the cholesterol molecule (387 Da), we count only the mass of its 7-carbon long alkyl chain (~ 99 Da). For the PEG_{2000}-DSPE lipid-polymer conjugate (2790 Da), we include its two 17-carbon long alkyl chains (~ 478 Da for both chains). For the ionizable lipid (640 Da), we count only the mass of its two 7-carbon long alkyl chains (~ 198 Da for both chains). For the DSPC molecule (790 Da), we count only the two 17-carbon long alkyl chains (~ 478 Da for both chains). For the PEG_{2000}-DMG lipid-polymer conjugate (2493 Da), we include its two 14-carbon long alkyl chains (~ 394 Da for both chains). For the PC molecule (775 Da), we only include its two 14-carbon long alkyl chains (~ 394 Da for both chains). For the PEG_{2000}-PE lipid-polymer conjugate (2693 Da), we include its two 13-carbon long alkyl chains (~ 366 Da for both chains). For the DPPC molecule (734 Da), we include its two 15-carbon long alkyl chains (~ 422 Da for both chains).

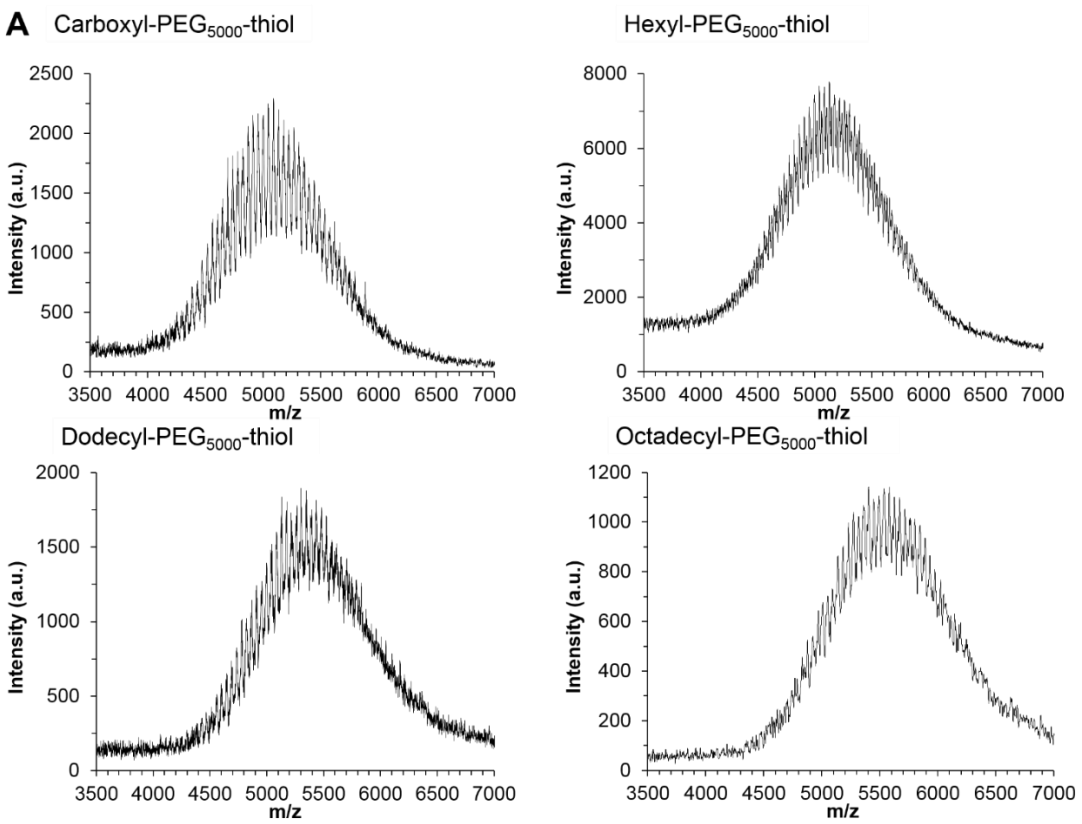

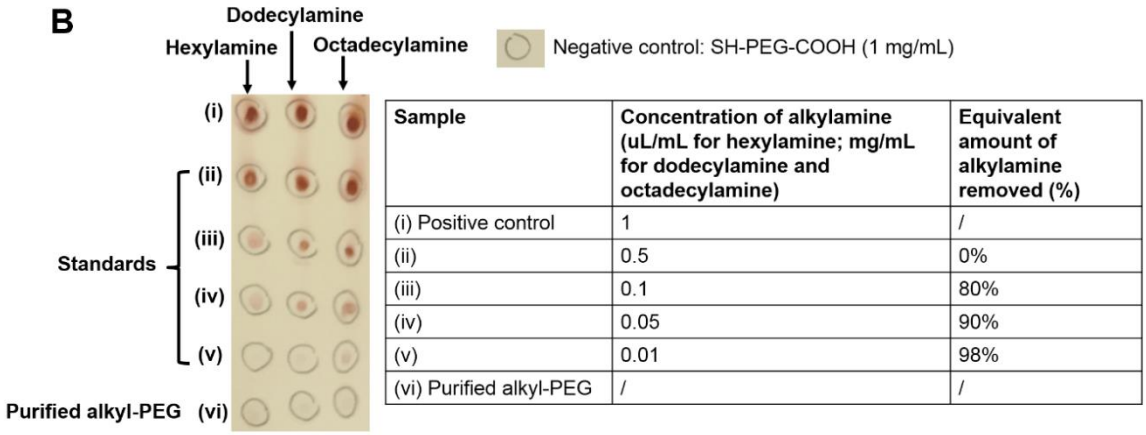

Sample	Concentration of alkylamine (uL/mL for hexylamine; mg/mL for dodecylamine and octadecylamine)	Equivalent amount of alkylamine removed (%)
(i) Positive control	1	/
(ii)	0.5	0%
(iii)	0.1	80%
(iv)	0.05	90%
(v)	0.01	98%
(vi) Purified alkyl-PEG	/	/

Figure S1. Characterization of alkyl-terminated and thiolated PEG (HS-PEG-C_nH_{2n+1}). (A) MALDI-TOF spectra of HS-PEG_{5000}-C_nH_{2n+1}. Covalent conjugation of alkylamine to carboxyl-PEG_{5000}-thiol leads to a right-shift of the peak of the MALDI-TOF spectra of hexyl-PEG_{5000}-thiol, dodecyl-PEG_{5000}-thiol, and octadecyl-PEG_{5000}-thiol. (B) A thin-layer chromatography (TLC) plate spotted with 10 μL of either alkylamine standards or our thus-synthesized alkyl-PEG-thiol was

immersed in ninhydrin solution. Emergence of purple color (Ruhemann's purple) indicates the presence of amines in the solution. After purification, almost 98% of the alkylamine initially introduced to the reaction was successfully removed from the PEG product (*i.e.,* alkyl-PEG-thiol), allowing us to exclude the possibility that the amine groups may interfere with the effect of alkylation on cellular uptake.

Table S2. Surface Plasmon Resonance (SPR) Peak of Alkyl$_{x\%}$-PEG-AuNPs as a Function of Alkyl Mole Percent (x%)

	SPR Peak (nm)				
	1%	**2%**	**4%**	**10%**	**100%**
Hexyl$_{x\%}$-PEG-AuNPs	524	524	524	525	527
Dodecyl$_{x\%}$-PEG-AuNPs	524	524	524	525	529
Octadecyl$_{x\%}$-PEG-AuNPs	522	523	523	530	532

Table S3. Hydrodynamic Sizes of Alkyl$_{4\%}$-PEG-AuNPs in Intensity, Number, and Volume

Sample	d_i (nm)[a]	d_n (nm)[b]	d_v (nm)[c]	Polydispersity index (PDI)
Citrate-capped AuNPs	27.1 ± 0.3	19.5 ± 1.4	23.6 ± 1.0	0.1
Methoxy-PEG-AuNPs	55.4 ± 0.8	32.2 ± 0.8	40.2 ± 0.8	0.2
Hexyl$_{4\%}$-PEG-AuNPs	55.3 ± 1.2	31.0 ± 1.2	39.1 ± 0.8	0.2
Dodecyl$_{4\%}$-PEG-AuNPs	54.4 ± 1.8	35.6 ± 0.4	40.0 ± 0.2	0.2
Octadecyl$_{4\%}$-PEG-AuNPs	49.7 ± 0.8	31.7 ± 0.2	38.2 ± 0.2	0.2

[a] Reported data represent mean ± SD from three independent measurements of hydrodynamic diameter in intensity (d_i).

[b] Reported data represent mean ± SD from three independent measurements of hydrodynamic diameter in number (d_n).

[c] Reported data represent mean ± SD from three independent measurements of hydrodynamic diameter in volume (d_v).

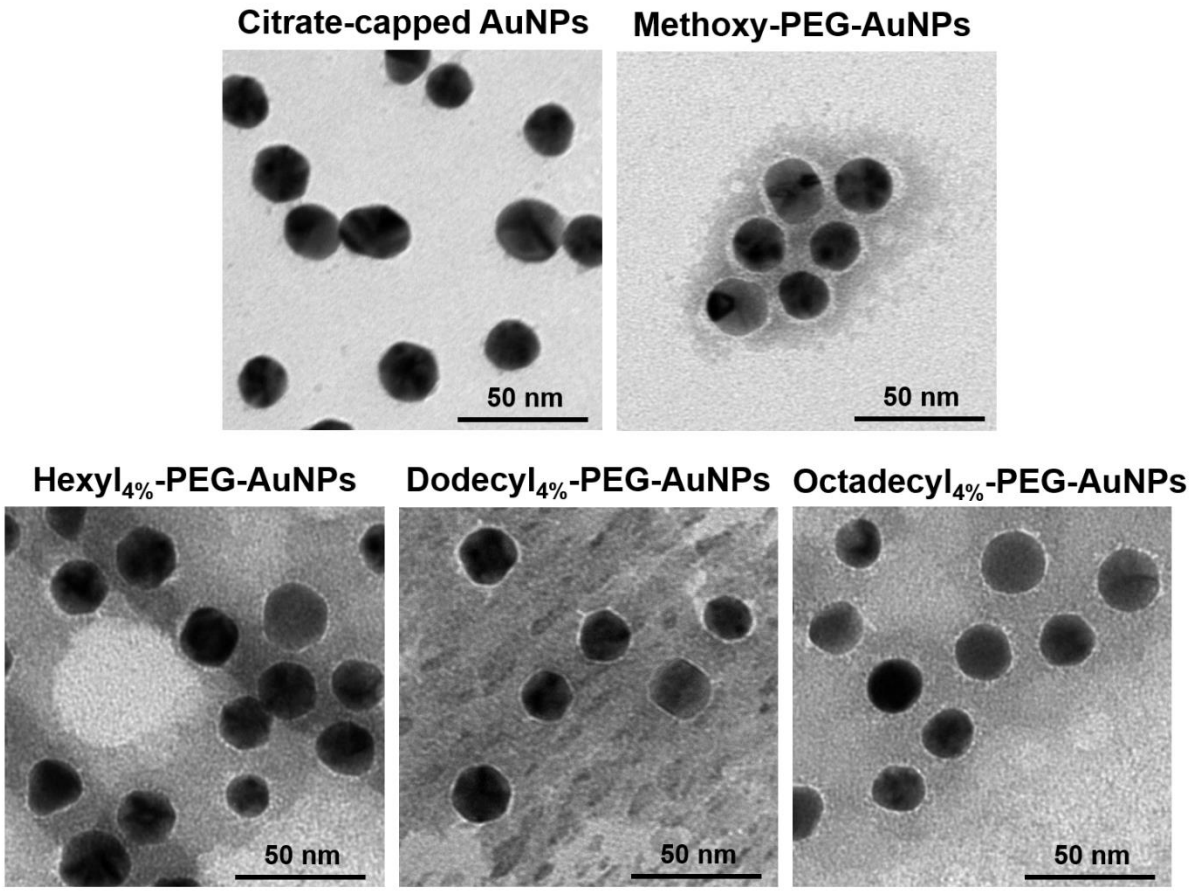

Figure S2. Representative TEM images of citrate-capped AuNPs, methoxy-PEG-AuNPs, hexyl$_{4\%}$-PEG-AuNPs, dodecyl$_{4\%}$-PEG-AuNPs, and octadecyl$_{4\%}$-PEG-AuNPs. Negative staining of methoxy-PEG-AuNPs and alkyl$_{4\%}$-PEG-AuNPs by uranyl acetate reveals the PEG shell of ~ 2.5 nm thick around the AuNP core, in agreement with the TEM images of the same groups of AuNPs negatively stained by phosphotungstic acid (PTA) as shown in Figure 1 in the main text.

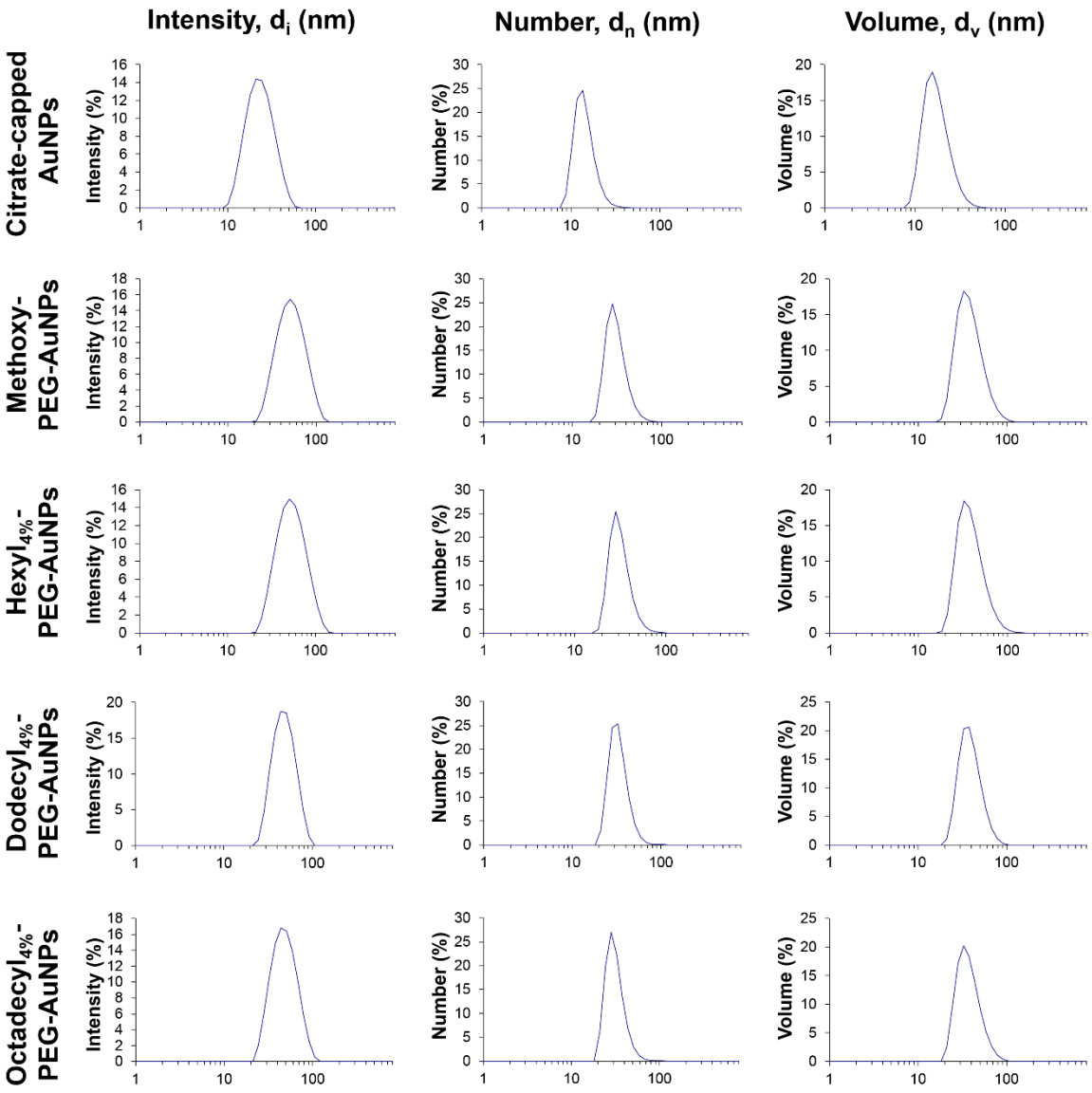

Figure S3. DLS profiles for alkyl$_{4\%}$-PEG-AuNPs. DLS profiles of hydrodynamic diameter of alkyl$_{4\%}$-PEG-AuNPs in intensity (left; d_i), number (middle; d_n), and volume (right; d_v).

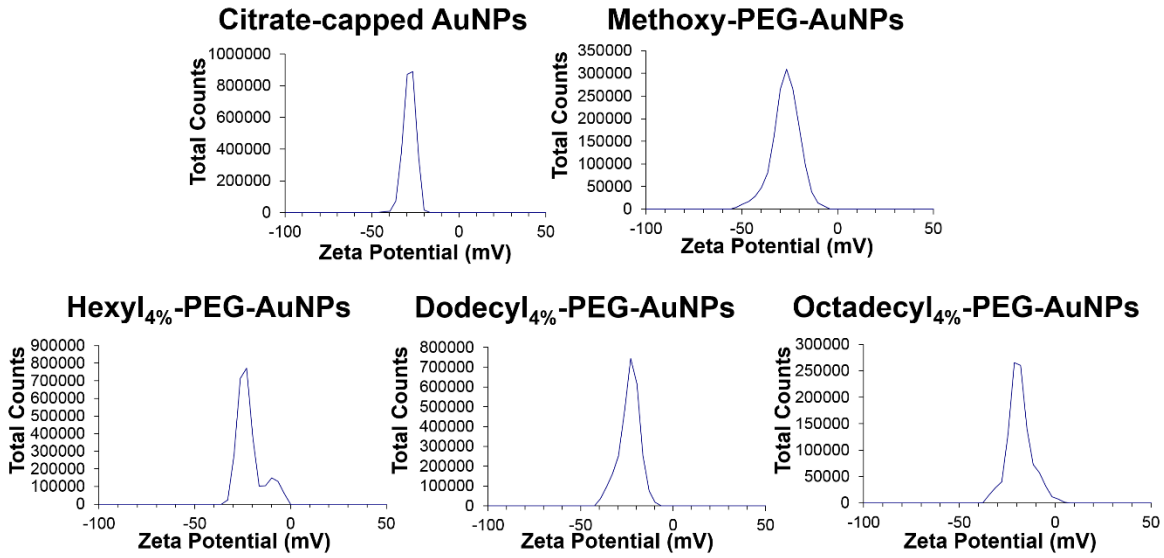

Figure S4. Zeta potential profiles for citrate-capped AuNPs, methoxy-PEG-AuNPs, and alkyl$_{4\%}$-PEG-AuNPs.

Table S4 Mass Percentage of Alkyl Groups in the total PEG Coating of Alkyl-PEG-AuNPs

A: Mole percentage of alkyl-PEG in the total PEG coating in different classes of alkyl-PEG-AuNPs (%)	B: No. of alkyl-PEG strands per NP (B = Total no. of PEG strands per NP[a] × A)	C: Mass of each alkyl group (Da)	D: Mass of total alkyl groups per NP (D = B × C) (Da)	E: Mass percentage of alkyl groups in the total PEG coating (E = D/(5000 × 4500) × 100%) (%)[b]
Hexyl$_{x\%}$-PEG-AuNPs				
1 mol%	45	85 Da	3825 Da	0.02%
1.3 mol%	60	85 Da	5100 Da	0.02%
2 mol%	90	85 Da	7650 Da	0.03%
4 mol%[c]	180	85 Da	15300 Da	0.07%
10 mol%	450	85 Da	38250 Da	0.17%
100 mol%	4500	85 Da	382500 Da	1.67%
Dodecyl$_{x\%}$-PEG-AuNPs				
1 mol%	45	169 Da	7605 Da	0.03%
1.3 mol%	60	169 Da	10140 Da	0.05%
2 mol%	90	169 Da	15210 Da	0.07%
4 mol%[c]	180	169 Da	30420 Da	0.14%
10 mol%	450	169 Da	76050 Da	0.34%
100 mol%	4500	169 Da	760500 Da	3.27%
Octadecyl$_{x\%}$-PEG-AuNPs				
1 mol%	45	253 Da	11385 Da	0.05%
1.3 mol%	60	253 Da	15180 Da	0.07%
2 mol%	90	253 Da	22770 Da	0.10%
4 mol%[c]	180	253 Da	45540 Da	0.20%
10 mol%	450	253 Da	113850 Da	0.50%
100 mol%	4500	253 Da	1138500 Da	4.82%

[a] The total no. of PEG strands (alkyl-PEG and mPEG) per NP is around 4500 (Table 2).

[b] Mass percentage of alkyl groups out of the total PEG coating $= \frac{\text{(Mass of alkyl group)} \times \text{(Total number of alkyl-terminated PEG strands)}}{\text{(Mass of PEG)} \times \text{(Total number of alkyl- and methoxy-terminated PEG stands)}} \times 100\%$

[c] We use a 4 mol% alkyl-PEG for most of our cellular uptake and intracellular trafficking studies (highlighted in yellow).

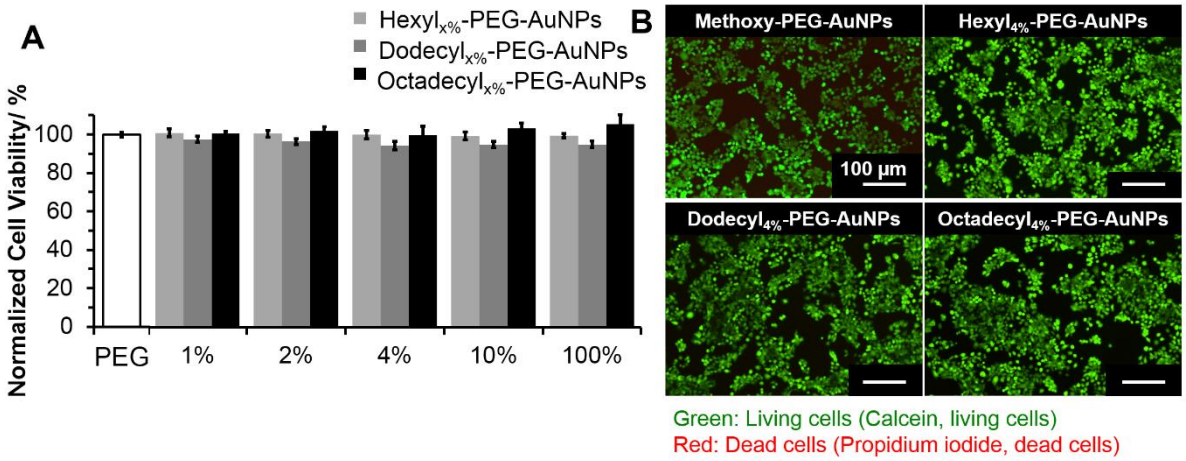

Figure S5. Cytotoxicity of alkyl-PEG-AuNPs. (A) Kera-308 cells were incubated with PEG-AuNPs that contain different molar ratios of alkyl groups to methoxy groups (*i.e.,* alkyl$_{x\%}$-PEG-AuNPs) in the PEG coating. By the alamarBlue assay, the treated cells remain largely viable after incubation with 1 nM NPs for 24 h. Error bar denotes the standard deviation resulting from four experiments. (B) After incubation with 1 nM methoxyl-PEG-AuNPs or alkyl$_{4\%}$-PEG-AuNPs of different carbon chain lengths for 24 h, the Kera-308 cells were stained with calcein-AM (a chemical stain for living cells; green) and propidium iodide (a chemical stain for dead cells; red). By fluorescence microscopy, most treated cells remain viable (green).

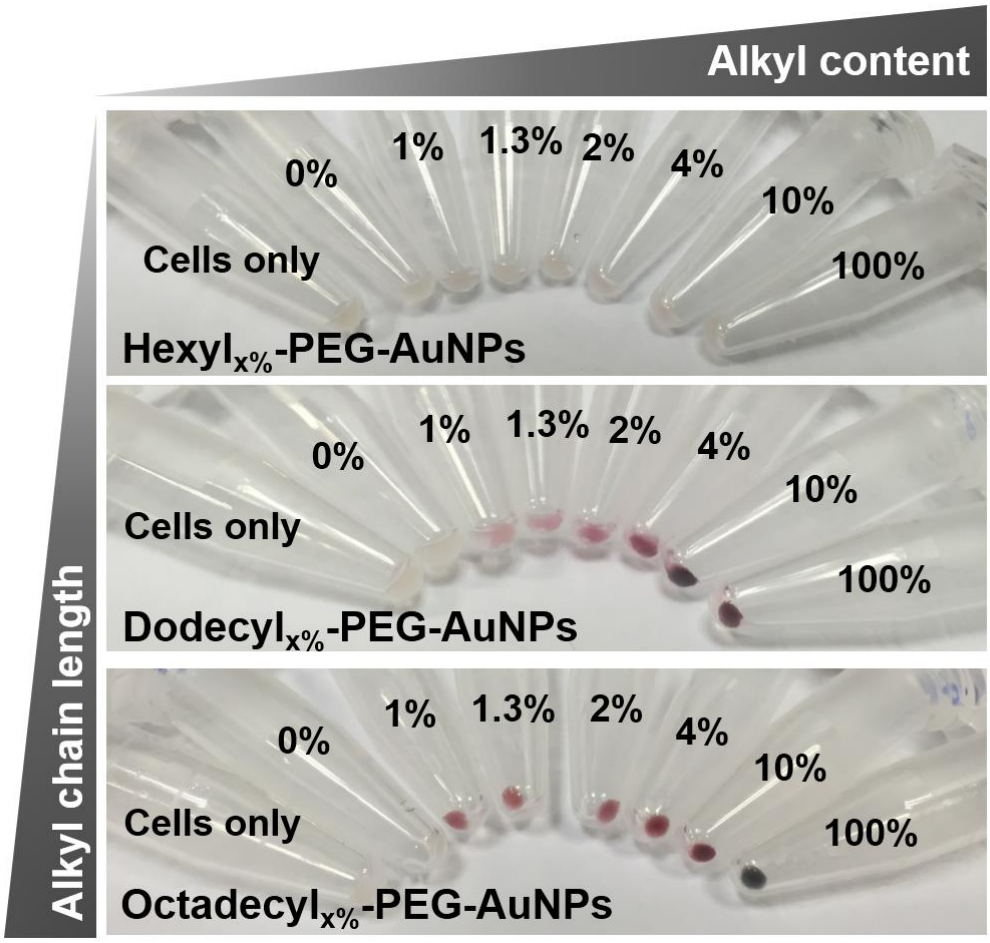

Figure S6. Kera-308 cells (mouse keratinocytes) were incubated with 1 nM either methoxy-PEG-AuNPs or alkyl$_{x\%}$-PEG-AuNPs containing 1%, 1.3%, 2%, 4%, 10%, and 100% (all in terms of mol%) hexyl, dodecyl, or octadecyl groups in the PEG coating for 24 h. The corresponding ICP-MS data for these cell pellets are shown in Figure 2A. The cell pellets reveal a strong dependence of cellular association on the carbon chain length and amount of alkyl chains in the PEG coating, as seen by the enormous variation in the red color due to the surface plasmon resonance of AuNPs.

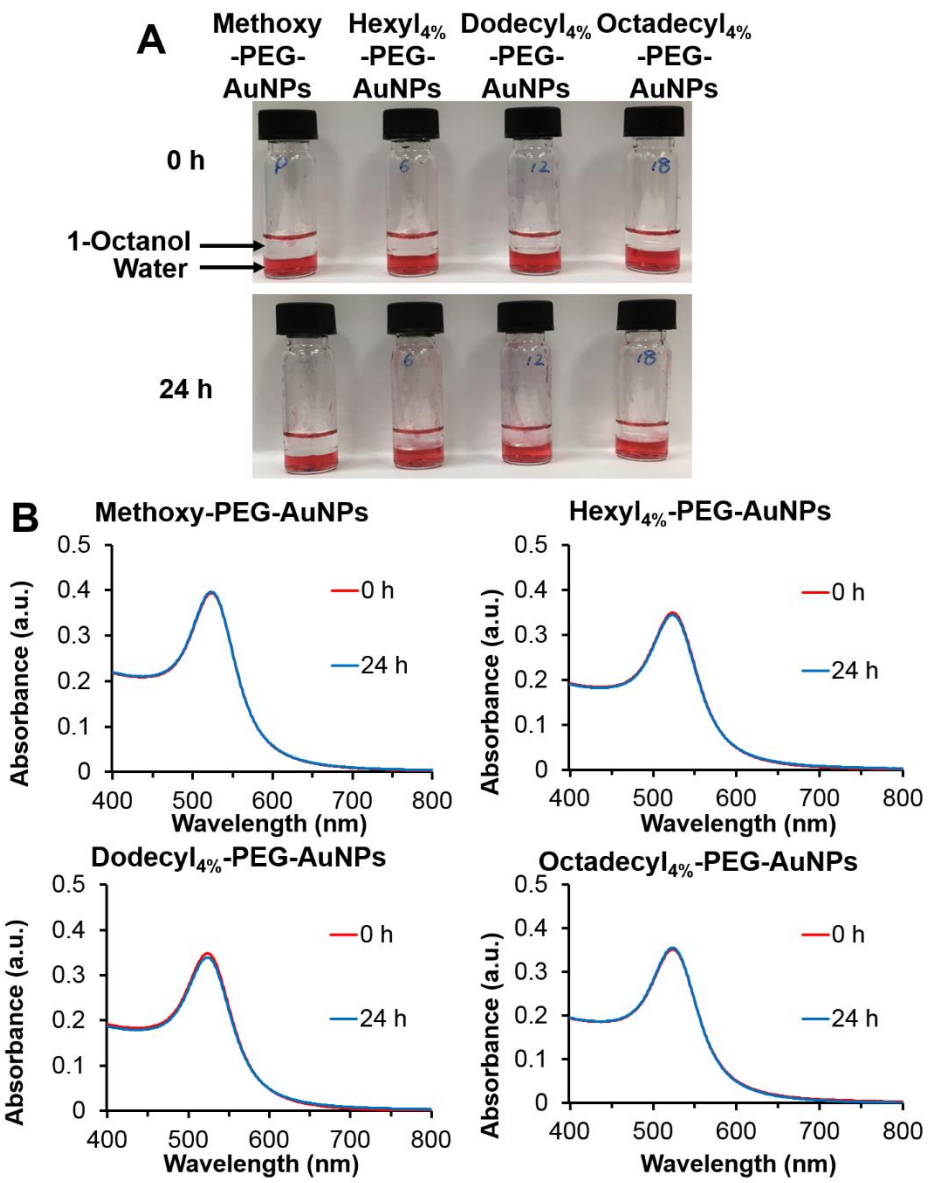

Figure S7. 1-Octanol/water partitioning experiment of methoxy-PEG-AuNPs and alkyl$_{4\%}$-PEG-AuNPs. (A) Methoxy-PEG-AuNPs and alkyl$_{4\%}$-PEG-AuNPs do not show observable transfer from water to 1-octanol after 24 h of mixing. Upper layer: 1-octanol; Lower layer: water. (B) The UV-vis spectra of NPs in water after 24 h of mixing. There is insignificant drop in the concentration of NPs in water, indicating limited transfer from water to 1-octanol.

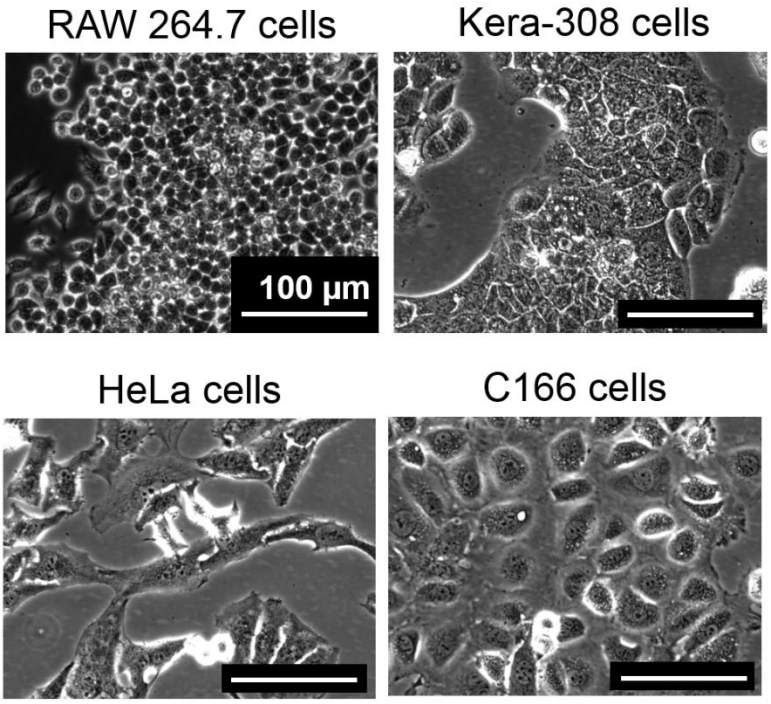

Figure S8. Representative microscopic images of RAW 264.7 (mouse macrophage), Kera-308 (mouse keratinocyte), HeLa (human cervical cancer), and C166 (mouse endothelial) cells.

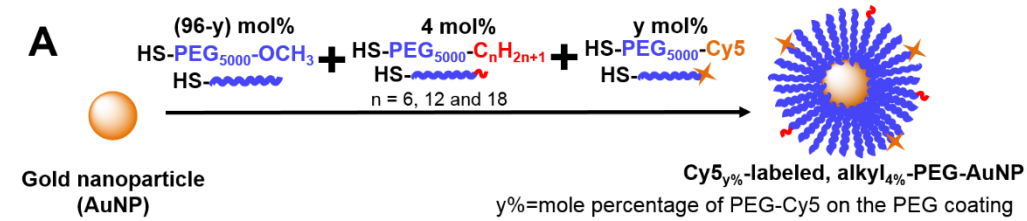

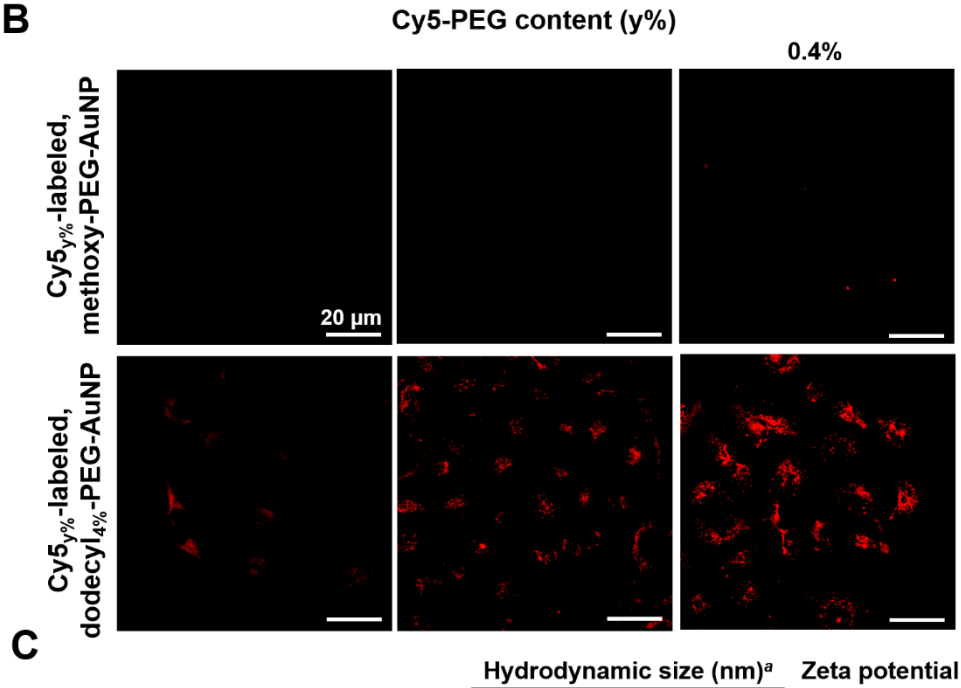

C

Sample	Hydrodynamic size (nm)[a] Water	Hydrodynamic size (nm)[a] OptiMEM	Zeta potential (mV)[b]
$Cy5_{0.13\%}$-labeled, methoxy-PEG-AuNPs	41.4 (0.2)	45.8 (0.2)	-17.4
$Cy5_{0.13\%}$-labeled, $hexyl_{4\%}$-PEG-AuNPs	40.8 (0.2)	39.7 (0.2)	-25.9
$Cy5_{0.13\%}$-labeled, $dodecyl_{4\%}$-PEG-AuNPs	44.2 (0.2)	83.0 (0.2)	-20.7
$Cy5_{0.13\%}$-labeled, $octadecyl_{4\%}$-PEG-AuNPs	45.1 (4.1)	124.1 (0.3)	-21.3

[a] Reported data represent mean from three independent measurements of Z-average size. Bracketed number refers to polydispersity index (PDI).
[b] Reported data represent mean from three independent measurements.

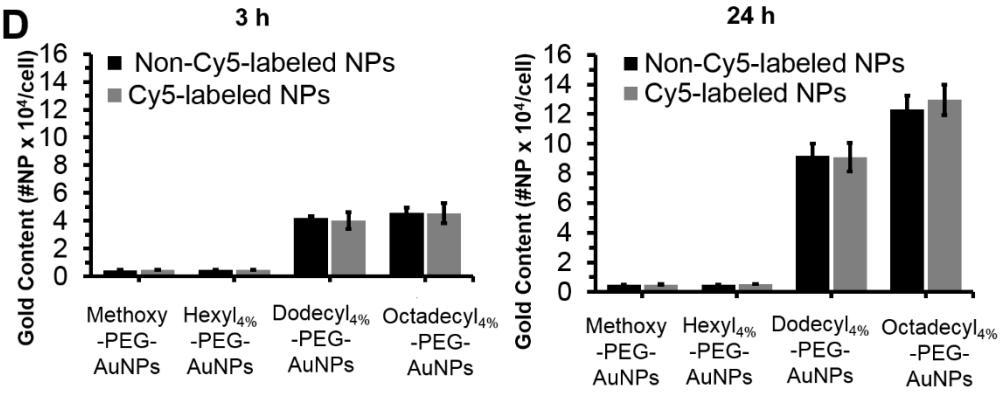

Figure S9. Preparation of Cy5-tagged dodecyl$_{4\%}$-PEG-AuNPs. (A) Preparation of alkyl$_{4\%}$-PEG-Cy5$_{y\%}$-AuNPs. Different mole ratios of alkyl-terminated PEG-thiol (HS-PEG-alkyl; 4 mol%), Cy5-terminated PEG-thiol (HS-PEG-Cy5; y mol%), and methoxy-terminated PEG-thiol [HS-PEG-OCH_3; (96-y) mol%] are coupled to the surface of citrate-capped AuNPs *via* gold-sulfur linkages. (B) Kera-308 cells were incubated with 1 nM Cy5-tagged methoxyl-PEG-AuNPs or Cy5-tagged dodecyl$_{4\%}$-PEG-AuNPs for 24 h. By confocal imaging, Cy5-tagged methoxy-PEG-AuNPs uptake do not enter the cell in detectable amounts for all Cy5 contents tested (0.13 mol%, 0.2 mol%, and 0.4 mol%). By contrast, we observed intense intracellular Cy5 fluorescence signals (red) that result from the efficient cellular entry of Cy5-tagged dodecyl$_{4\%}$-PEG-AuNPs. As expected, these Cy5 signals increase with increasing number of Cy5 strands covalently attached to the NP. The presence of Cy5 groups does not trigger the endocytosis of PEG-coated AuNPs. Based on these studies, we opted for the incorporation of 0.13 mol% of Cy5-PEG strands onto the PEG coating of AuNPs. (C) By dynamic light scattering, the hydrodynamic size of the Cy5-labeled alkyl$_{4\%}$-PEG-AuNPs in water is similar to that of the non-fluorescent alkyl$_{4\%}$-PEG-AuNPs, hovering in the range of 40-50 nm (refer to Table 2). Likewise, the Cy5-labeled NPs and their non-fluorescent sizes analogs also share similar sizes after incubation in OptiMEM at 37˚C for 24 h (refer to Table 3). The ζ-potentials of the Cy5-labeled NPs are similar to those of the unlabeled alkyl$_{4\%}$-PEG-AuNPs ranging between -24 mV to -17 mV as indicated in Table 2. (D) Kera-308 cells were incubated with 1 nM of Cy5$_{0.13\%}$-labeled or non-Cy5-labeled alkyl$_{4\%}$-PEG-AuNPs for 3 h and 24 h. By ICP-MS measurements, the cellular association of Cy5-labeled NPs is not significantly different from that of the non-Cy5-labeled NPs.

Table S5. Hydrodynamic Sizes of Alkyl$_{4\%}$-PEG-AuNPs in Intensity, Number, and Volume in Different Media.

	Hydrodynamic size of alkyl$_{4\%}$-PEG-AuNPs (nm)[a]				
	Water	**PBS[b]**	**OptiMEM**	**DMEM + 0% FBS[c]**	**DMEM + 10% FBS**
Methoxy-PEG-AuNPs					
d_i	55.4 ± 0.8	102.5 ± 42.8	53.1 ± 0.7	196.4 ± 13.7	88.0 ± 43.7
d_n	32.2 ± 0.8	30.0 ± 2.3	36.3 ± 0.9	26.0 ± 2.4	32.4 ± 1.2
d_v	40.2 ± 0.8	92.1 ± 46.8	46.3 ± 6.5	50.8 ± 7.6	72.8 ± 56.0
PDI[d]	0.2	0.2	0.2	0.2	0.4
Hexyl$_{4\%}$-PEG-AuNPs					
d_i	55.3 ± 2.0	193.4 ± 39.7	75.9 ± 42.6	204.2 ± 55.9	103.5 ± 41.6
d_n	31.0 ± 1.2	32.5 ± 2.1	30.0 ± 4.5	98.3 ± 13.5	33.9 ± 4.2
d_v	39.1 ± 0.8	228.5 ± 38.9	67.7 ± 53.3	23.4 ± 6.5	109.7 ± 55.6
PDI[d]	0.2	0.1	0.2	0.2	0.3
Dodecyl$_{4\%}$-PEG-AuNPs					
d_i	54.5 ± 1.8	202.1 ± 50.7	68.0 ± 23.3	112.9 ± 80.0	213.5 ± 7.0
d_n	33.6 ± 0.4	34.0 ± 1.0	32.9 ± 1.8	30.7 ± 1.1	28.0 ± 4.1
d_v	40.0 ± 0.2	262.9 ± 43.8	45.6 ± 2.6	112.9 ± 80.0	53.9 ± 5.9
PDI[d]	0.2	0.1	0.3	0.2	0.5
Octadecyl$_{4\%}$-PEG-AuNPs					
d_i	49.7 ± 0.8	323.8 ± 40.7	77.2 ± 11.5	261.9 ± 53.0	271.9 ± 23.7
d_n	31.7 ± 0.2	27.46 ± 4.7	35.7 ± 1.8	100.1 ± 13.2	46.4 ± 18.7
d_v	38.2 ± 0.2	517.4 ± 25.0	48.1 ± 3.6	373.4 ± 59.8	130.6 ± 55.8
PDI[d]	0.2	0.4	0.2	0.2	0.4

[a] Reported data represent mean ± SD from three independent measurements in intensity (d_i), number (d_n), and volume (d_v).

[b] PBS = phosphate-buffered saline

[c] FBS = fetal bovine serum

[d] PDI = polydispersity index

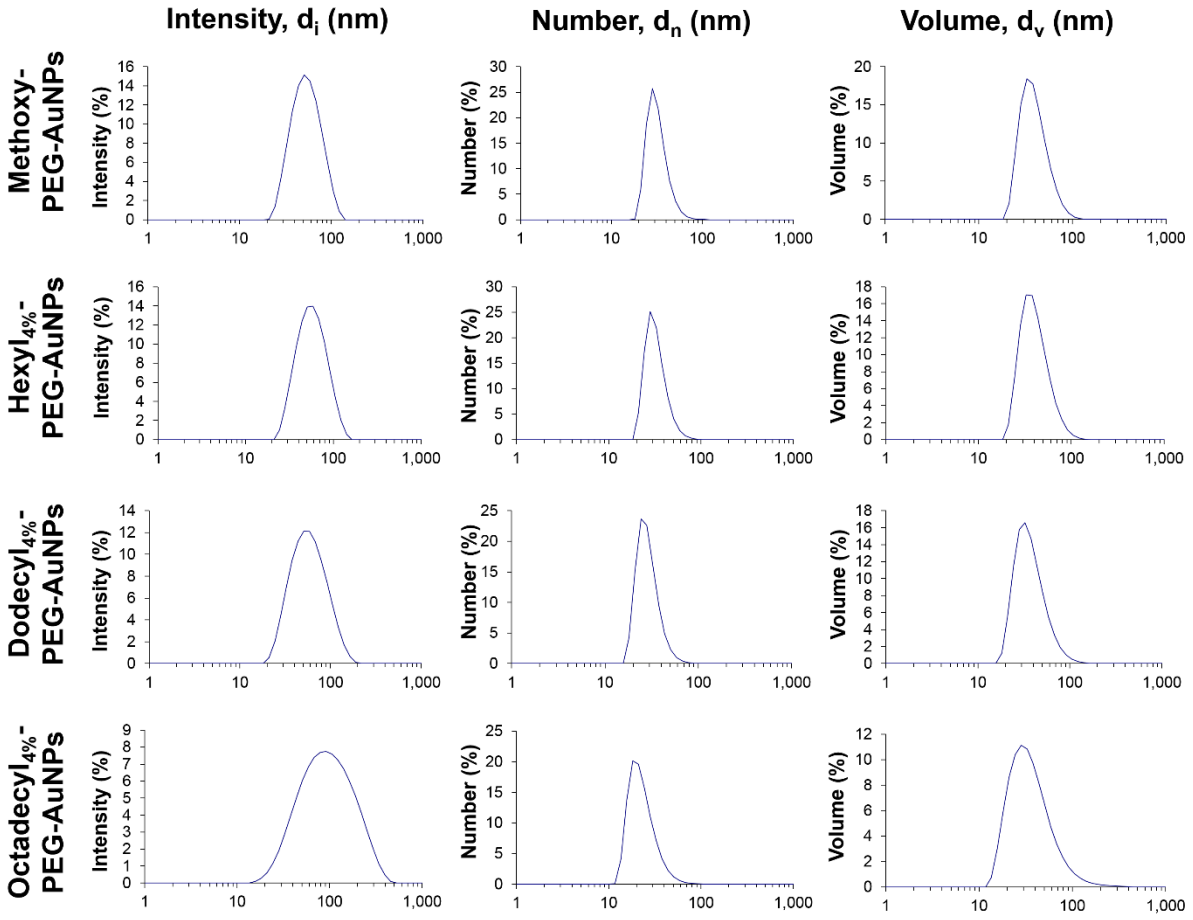

Figure S10. DLS profiles for alkyl$_{4\%}$-PEG-AuNPs in PBS. DLS profiles of hydrodynamic diameter of alkyl$_{4\%}$-PEG-AuNPs in intensity (left; d_i), number (middle; d_n), and volume (right; d_v).

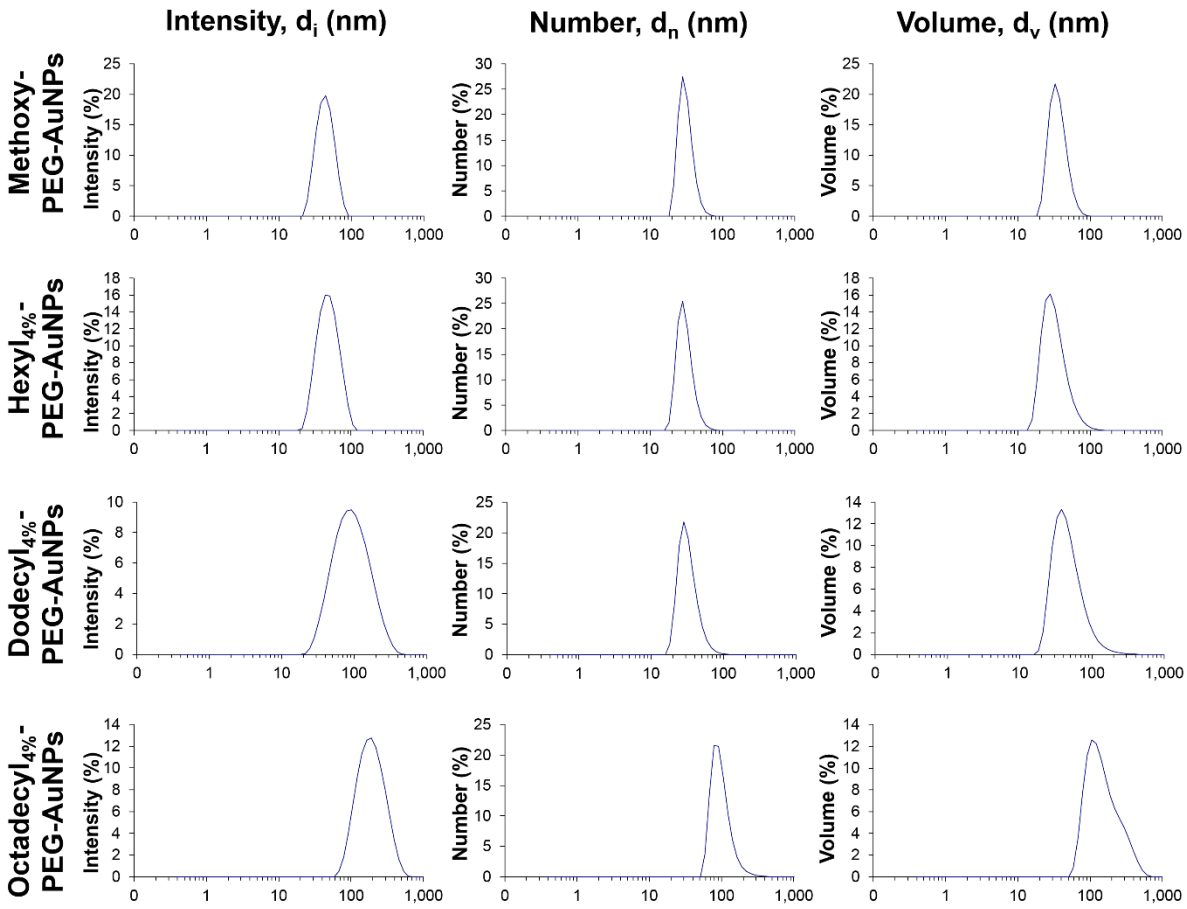

Figure S11. DLS profiles for alkyl$_{4\%}$-PEG-AuNPs in OptiMEM. DLS profiles of hydrodynamic diameter of alkyl$_{4\%}$-PEG-AuNPs in intensity (left; d_i), number (middle; d_n), and volume (right; d_v).

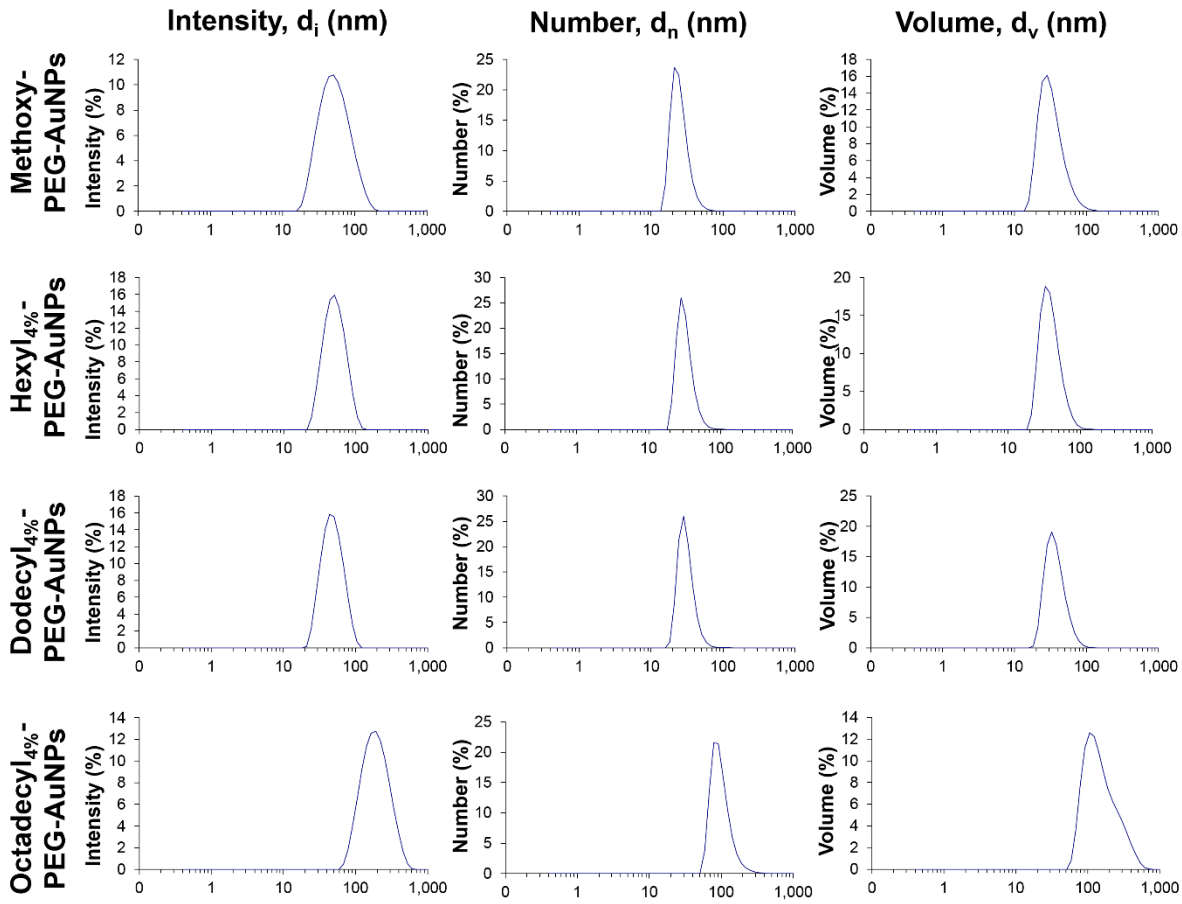

Figure S12. DLS profiles for alkyl$_{4\%}$-PEG-AuNPs in DMEM without FBS. DLS profiles of hydrodynamic diameter of alkyl$_{4\%}$-PEG-AuNPs in intensity (left; d_i), number (middle; d_n), and volume (right; d_v).

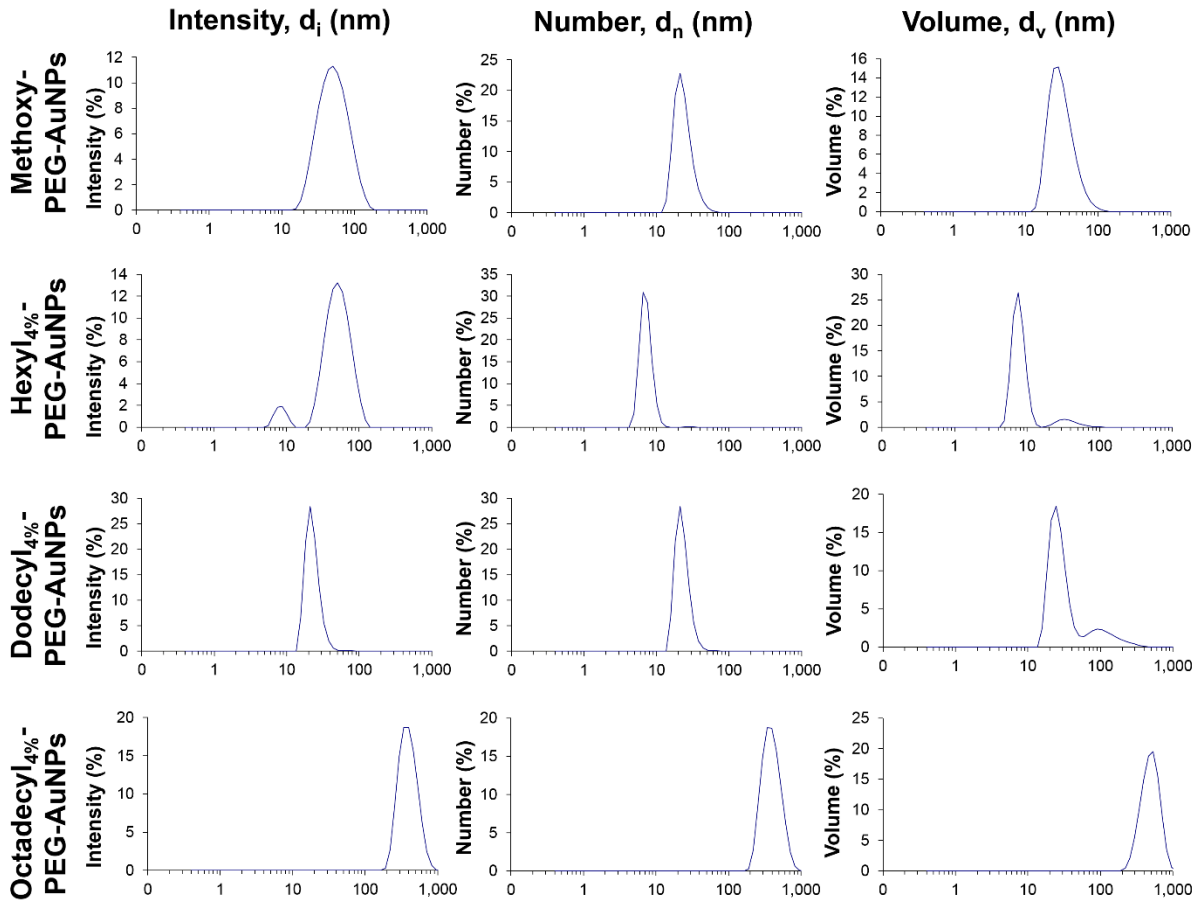

Figure S13. DLS profiles for alkyl$_{4\%}$-PEG-AuNPs in DMEM with 10% FBS. DLS profiles of hydrodynamic diameter of alkyl$_{4\%}$-PEG-AuNPs in intensity (left; d_i), number (middle; d_n), and volume (right; d_v).

A

	SPR Peak (nm)						
	5 min	0.5 h	1 h	3 h	4 h	8 h	24 h
Methoxy-PEG-AuNPs	523	523	522	522	522	522	522
$Hexyl_{4\%}$-PEG-AuNPs	523	522	522	522	522	522	522
$Dodecyl_{4\%}$-PEG-AuNPs	521	520	520	520	520	521	522
$Octadecyl_{4\%}$-PEG-AuNPs	522	520	520	518	518	520	520

B

	SPR Peak (nm)			
	PBS	OptiMEM	DMEM + 0% FBS	DMEM + 10% FBS
Methoxy-PEG-AuNPs	522	522	522	522
$Hexyl_{4\%}$-PEG-AuNPs	522	522	522	523
$Dodecyl_{4\%}$-PEG-AuNPs	522	522	523	523
$Octadecyl_{4\%}$-PEG-AuNPs	523	520	523	522

C

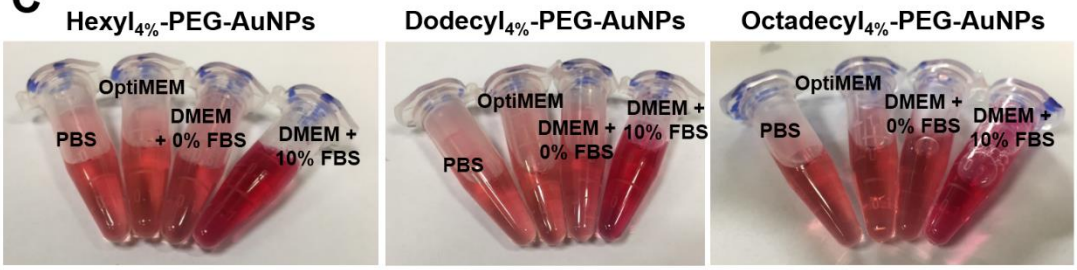

Figure S14. Effect of serum on the stability of alkyl-PEG-AuNPs. (A) Surface plasmon resonance (SPR) peak of methoxy-PEG-AuNPs and $alkyl_{4\%}$-PEG-AuNPs incubated in OptiMEM at 37˚C as a function of time. No significant red-shift in the SPR peaks of the AuNPs was observed for all carbon chain lengths tested, supporting the lack of large-scale aggregation of alkyl-PEG-AuNPs in OptiMEM across the 24-h incubation time window. (B and C) Upon incubation in PBS, OptiMEM, DMEM without FBS, and DMEM with 10% FBS at 37˚C for 24 h, 1 nM $alkyl_{4\%}$-PEG-AuNPs did not show significant red-shift in the SPR peaks and did not suffer from noticeable aggregation, as seen by the general red color of the AuNPs and the lack of large NP aggregates sedimenting to the bottom of the tubes.

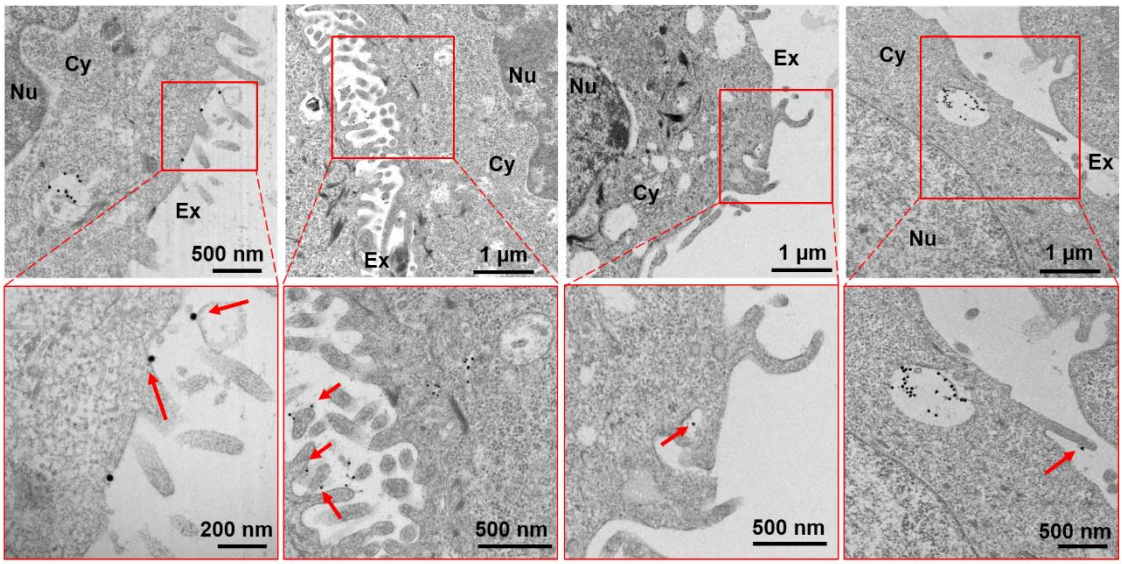

Figure S15. Extra TEM images capture the engagement of dodecyl$_{4\%}$-PEG-AuNPs by the filopodia (red arrows) of Kera-308 cells within the first 2 h of incubation, an observation similar to those cells incubated with dodecyl$_{4\%}$-PEG-AuNPs as shown in Figure 5A of the main text. The incubation concentration was 1 nM. The bottom row shows the enlargement of the boxed areas in the top row. (Legend: Nu = nucleus; Cy = cytosol; and Ex = extracellular space.)

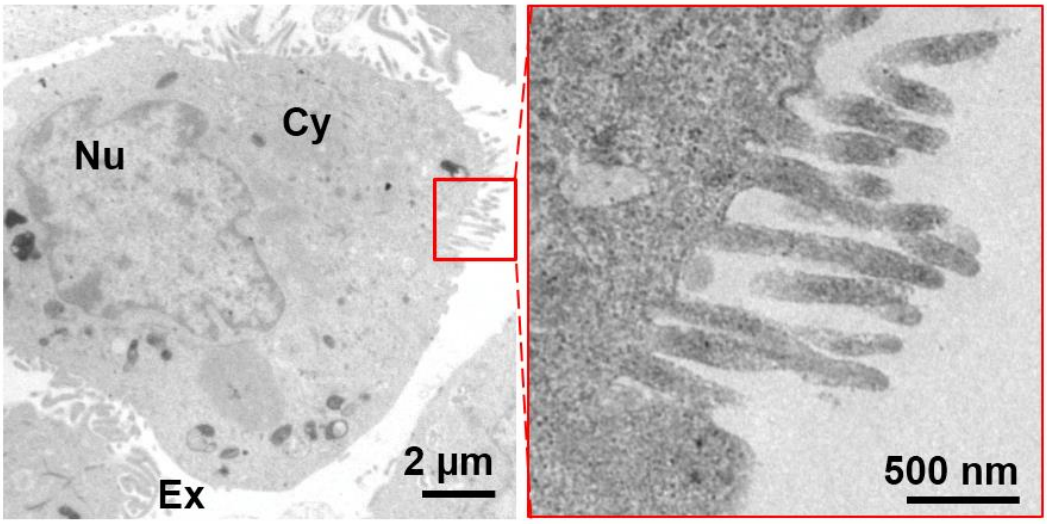

Figure S16. Extra TEM images of untreated Kera-308 cells show the abundance of filopodia that resemble those Kera-308 cells incubated with alkyl-PEG-AuNPs as shown in Figure 5A of the main text. The right image shows the enlargement of the boxed area in the left image. (Legend: Nu = nucleus; Cy = cytosol; and Ex = extracellular space.)

A

Treatment	Concentration	Pathway inhibited
4 °C	N.A.	Energy-dependent endocytosis
Methyl-β-Cyclodextrin (m-βCD)	10 mM	Lipid raft/caveolae, clathrin-dependent endocytosis and fluid phase endocytosis
Chlorpromazine	5 μg/mL	Clathrin-dependent endocytosis
Filipin III	2.5 μg/mL	Lipid raft/caveolae-dependent endocytosis
Amiloride	500 μg/mL	Macropinocytosis and phagocytosis
Mannan	1 mg/mL	Mannose receptor-mediated endocytosis
Fucoidan	50 μg/mL	Scavenger receptor-mediated endocytosis
Cytochalasin D	5 μg/mL	Macropinocytosis, phagocytosis, clathrin- or caveolae-dependent endocytosis
Dynasore	80 μM	Dynamin-dependent endocytosis

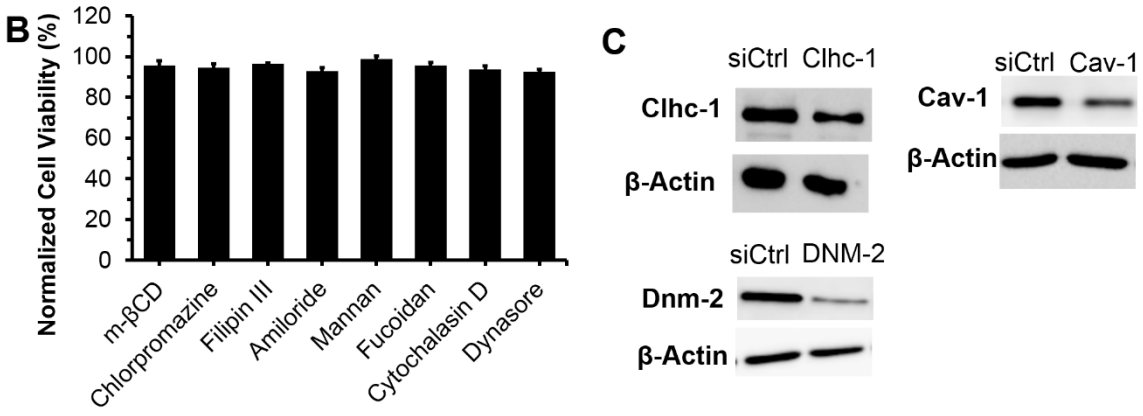

Figure S17. Pharmacological blocking and RNAi-mediated genetic knockdown in Kera-308 cells. (A) This table presents the pharmacological blockers used in the experiments featured in Figure 5B of the main text, together with their applied concentrations and intended pathways of cellular uptake. (B) Upon incubation with different blockers for 6 h, the treated Kera-308 cells remain largely viable by the alamarBlue assay. Error bar denotes the standard deviation resulting from four experiments. (C) Western blotting confirms the successful genetic knockdown of dynamin-2 (Dnm-2), caveolin-1 (Cav-1), and clathrin heavy chain 1 (Clhc-1) *via* RNA interference in Kera-308 cells. β-Actin was used as the house-keeping gene.

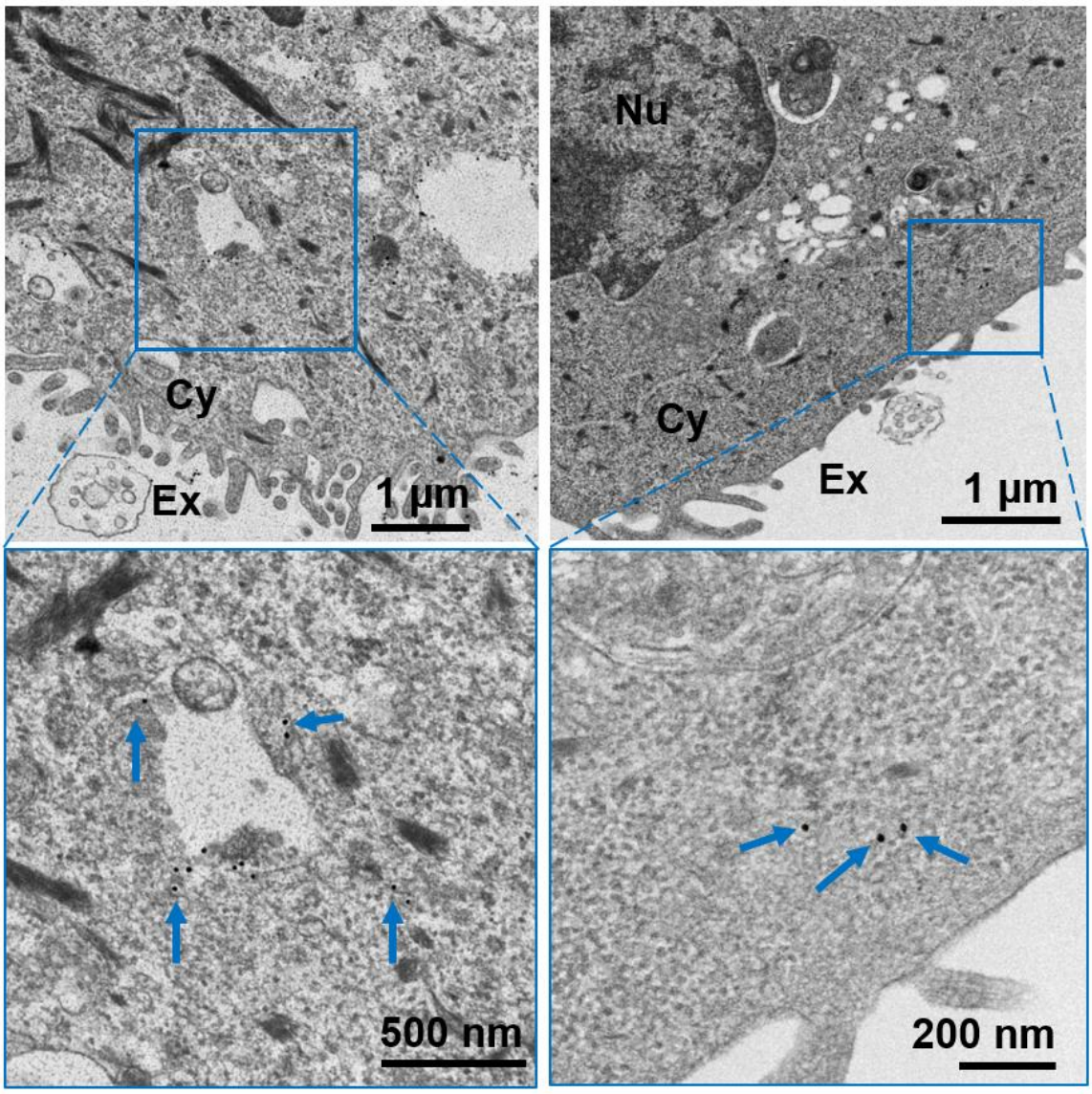

Figure S18. Extra TEM images capture the localization of dodecyl$_{4\%}$-PEG-AuNPs in the cytosol (blue arrows) of Kera-308 cells within the first 2 h incubation, an observation in a similar vein to those cells incubated with dodecyl$_{4\%}$-PEG-AuNPs as shown in Figure 6A of the main text. The bottom row shows the enlargement of the boxed areas in their top row. (Legend: Nu = nucleus; Cy = cytosol; and Ex = extracellular space.)

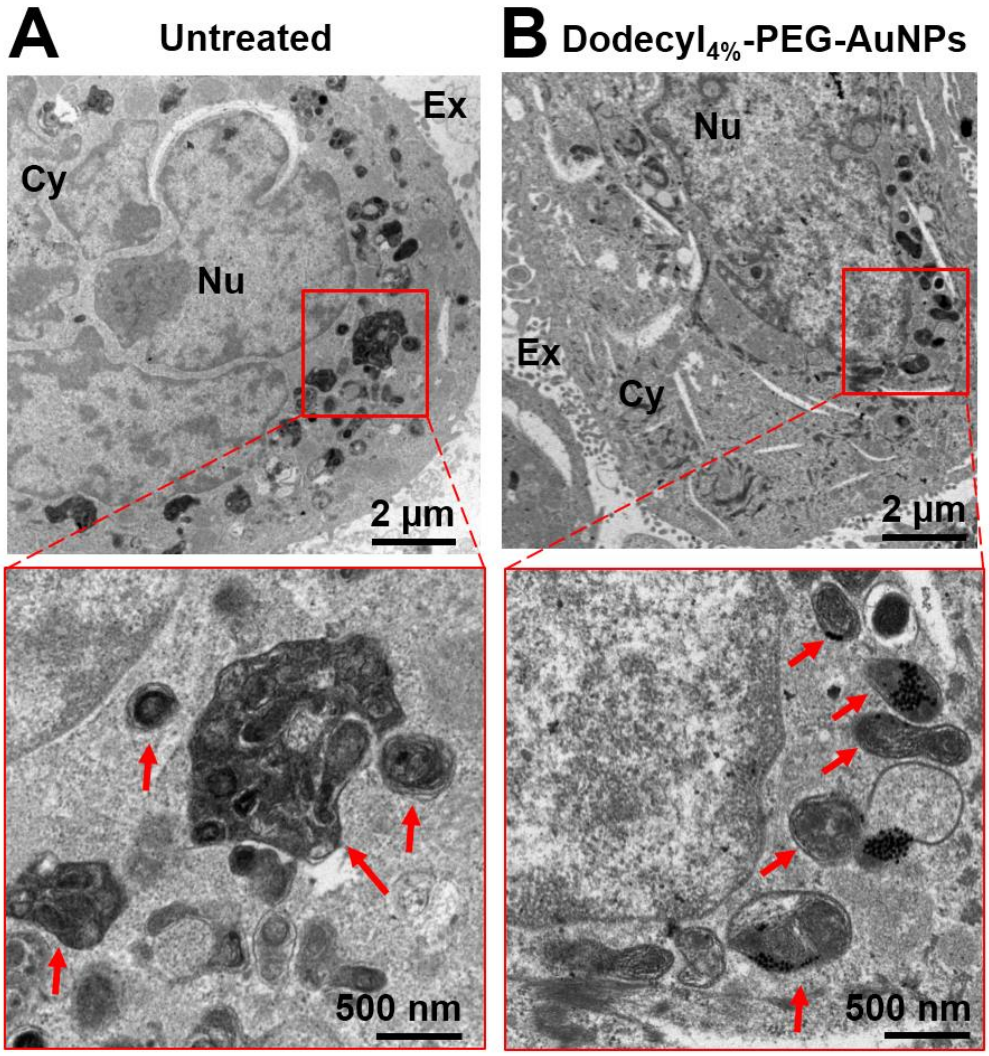

Figure S19. Additional TEM images of Kera-308 cells reveal the presence of lysosomes, as evidenced by the electronically-dense vesicles (red arrows) with multilamellar bodies (MLBs). Importantly, we detected MLBs in both (A) untreated cells and (B) cells that were incubated with 1 nM dodecyl$_{4\%}$-PEG-AuNPs for 24 h. The bottom row shows the enlargement of the boxed areas in their top row. The intracellular localization of the dodecyl$_{4\%}$-PEG-AuNPs in Figure S10A closely resembles that featured in Figure 6C of the main text. (Legend: Nu = nucleus; Cy = cytosol; and Ex = extracellular space.)

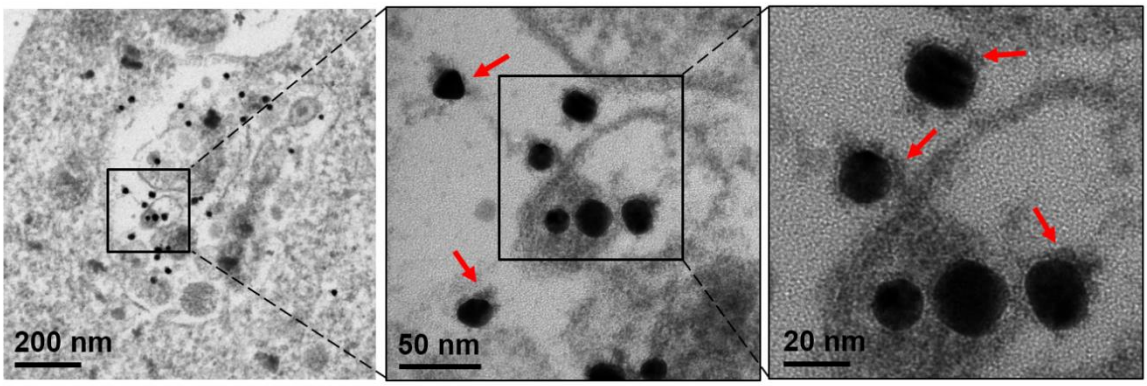

Figure S20. High-magnification TEM images capture the accumulation of dodecyl$_{4\%}$-PEG-AuNPs internalized by Kera-308 cells after 24 h of incubation. The NPs are in discrete form without colloidal aggregation in the intracellular compartment. The dense PEG coating of the NPs underwent minimal degradation as evidenced by the positively stained 5 nm shell by osmium tetroxide. The right images show the enlargement of the boxed areas on their left.

REFERENCES

1. Ishida, T.; Ichihara M.; Wang X. Y.; Yamamoto K.; Kimura J.; Majima E., Kiwada H. Injection of PEGylated Liposomes in Rats Elicits PEG-Specific IgM, which is Responsible for Rapid Elimination of Second Dose of PEGylated Liposomes. *J. Control Release*. **2006**, 112, 15-25.

2. Gilleron, J.; Querbes, W.; Zeigerer, A.; Borodovsky, A.; Marsico, G.; Schubert, U.; Manygoats, K.; Seifert, S.; Andree, C.; Stoter, M. ; Epstein-Barash, H.; Zhang, L. G.; Koteliansky, V.; Fitzgerald, K.; Fava, E.; Bickle, M.; Kalaidzidis, Y.; Akinc, A.; Maier, M.; Zerial, M.; Image-Based Analysis of Lipid Nanoparticle-Mediated siRNA Delivery, Intracellular Trafficking and Endosomal Escape. *Nat. Biotechnol.* **2013**, *31*, 638-646.

3. Sengupta, P.; Basu, S.; Soni, S.; Pandey, A.; Roy, B.; Oh, M. S.; Chin, K. T.; Paraskar, A. S.; Sarangi, S.; Connor, Y.; Sabbisetti, V. S.; Kopparam, J.; Kulkarni, A.; Muto, K.; Amarasiriwardena, C.; Jayawardene, I.; Lupoli, N.; Dinulescu, D. M.; Bonventre, J. V.; Mashelkar, R. A.; *et al.* Cholesterol-Tethered Platinum II-Based Supramolecular Nanoparticle Increases Antitumor Efficacy and Reduces Nephrotoxicity. *Proc. Natl. Acad. Sci. U.S.A.* **2012**, *109*, 11294-11299.

4. Dubertret, B.; Skourides, P.; Norris, D. J.; Noireaux, V.; Brivanlou, A. H.; Libchaber, A. *In vivo* Imaging of Quantum Dots Encapsulated in Phospholipid Micelles. *Science.* **2002**, 298, 1759-1762.